Procaine induces cell cycle arrest, apoptosis and autophagy through the inhibition of the PI3K/AKT and ERK pathways in human tongue squamous cell carcinoma

MIAO HAO[1*], CHU ZHANG[2,3*], NAIXU SHI[2], LIN YUAN[2], TIANFU ZHANG[2] and XIAOFENG WANG[2]

[1]Scientific Research Center; [2]Department of Stomatology, China-Japan Union Hospital of Jilin University, Changchun, Jilin 130033; [3]People's Hospital of Zhengzhou, Zhengzhou, Henan 450000, P.R. China

Received June 29, 2023; Accepted February 13, 2024

DOI: 10.3892/ol.2024.14541

Abstract. Procaine (PCA), a local anesthetic commonly used in stomatology, exhibits antitumor activity in some human malignancies. However, the precise mechanism underlying PCA activity remains unknown, and its antitumor effect in human tongue squamous carcinoma cells has not been reported. Flow cytometry and western blotting were used to assess the effects of PCA on mitochondrial membrane potential (ΔΨm), intracellular reactive oxygen species (ROS) production, cell cycle and apoptosis. The results suggested that PCA inhibits CAL27 and SCC-15 cell proliferation, and clone formation in a dose-dependent manner. CAL27 cells were more sensitive to PCA than SCC-15 cells. PCA also significantly inhibited cell migration, induced mitochondrial damage, reduced ΔΨm and increased intracellular ROS production. PCA causes G2/M cycle arrest and induces apoptosis. The possible mechanism for the inhibition of human tongue squamous carcinoma cell proliferation is through the regulation of ERK phosphorylation and PI3K/AKT-mediated signaling pathways. The results further suggested that autophagy occurs during PCA-induced apoptosis in CAL27 cells, and the addition of the autophagy inhibitor hydroxychloroquine sulfate further enhanced the sensitivity of PCA to inhibit cell proliferation, indicating that autophagy plays an important role in protecting cancer cells from apoptosis. PCA shows potential as an anticancer drug and its combination with autophagy inhibitors enhances its sensitivity.

Correspondence to: Professor Xiaofeng Wang, Department of Stomatology, China-Japan Union Hospital of Jilin University, 126 Xiantai Street, Changchun, Jilin 130033, P.R. China
E-mail: wangxiaofeng@jlu.edu.cn

*Contributed equally

Key words: tongue squamous carcinoma, procaine, cell cycle, apoptosis, autophagy

Introduction

Oral cancer is one of the most common cancers worldwide, and accounts for 4% of all cancer cases (1). Oral squamous cell carcinoma (OSCC) is the most common tumor that occurs in the oral and maxillofacial regions, causing marked mortality (2). At present, the main clinical treatments for OSCC are surgery, radiotherapy and chemotherapy (3). In 2020, 377,713 cases of OSCC were reported worldwide (4). The Global Cancer Observatory predicts that by 2040, the incidence of OSCC will increase by ~40%, with a concomitant increase in mortality, the overall 5-year survival rate of OSCC remains <50% (3,5,6). Considering the special physiological characteristics of the oral cavity, the treatment of OSCC not only emphasizes the improvement in the survival rate of patients, but also aims at improving their quality of life (7). However, the unique structural characteristics of the oral cavity make it complicated and challenging to complete postoperative reconstruction, which usually results in poor quality of life for patients (8). Therefore, it is evident that novel effective drugs for the treatment of OSCC are required.

Procaine (PCA) is a common local anesthetic drug mainly used in oral surgeries. Recent studies have shown that in addition to anesthesia, PCA has been proven to be an inhibitor of DNA methylation (9,10). Villar-Garea *et al* (11) found that PCA not only inhibited MCF-7breast cancer cell proliferation, but was also tightly bound to DNA rich in CpG islands, causing DNA demethylation events. In addition, a study indicated that PCA could inhibit the growth of liver cancer cells both *in vitro* and *in vivo,* and has a demethylation effect (12). Despite the fact that the antitumor effect of PCA has been partially studied, these studies have focused on the epigenetic effects of PCA, and have not explored the mechanism of cell proliferation inhibition by PCA. In particular, the mechanism of action of PCA in human oral tongue squamous cell carcinoma CAL27 cells is still unclear. Therefore, in the present study, the aim was to elucidate the effect of PCA on tongue squamous cell carcinoma. The potential mechanism of PCA as an anticancer drug in CAL27 cells was also studied. The results could provide novel ideas for the future applications of PCA as an antitumor drug in clinical treatment.

Materials and methods

Reagents. DMEM, fetal bovine serum (FBS) and penicillin/streptomycin were purchased from Gibco; Thermo Fisher Scientific, Inc. PCA (cat. no. 51-05-8) was purchased from Thermo Fisher Scientific, Inc. The anti-GAPDH (cat. no. 5174), anti-p21 (cat. no. 2947), anti-Bcl-2 (cat. no. 2870), anti-Bax (cat. no. 5023), anti-survivin (cat. no. 2808), anti-LC3B (cat. no. 3868), anti-p62 (cat. no. 8025), anti-ERK (cat. no. 9102), anti-phosphorylated (p)-ERK (cat. no. 4370), anti-AKT (cat. no. 9272), anti-p-AKT (cat. no. 4060) and anti-PI3K (cat. no. 4249) polyclonal antibodies were purchased from Cell Signaling Technology, Inc. IRDye 800CW goat anti-rabbit IgG (cat. no. 925-32211) was purchased from LI-COR Biosciences. Cell Counting Kit (CCK-8) was purchased from Dojindo Laboratories, Inc. Rhodamine 123, crystal violet dye and RIPA cell lysate were purchased from Beyotime Institute of Biotechnology. Western blotting protein prestaining marker, primers, β-actin, CDK2 and cyclin E were obtained from Shanghai Sangong Pharmaceutical Co., Ltd. Hydroxychloroquine sulfate (CQ) was purchased from Selleck Chemicals. The cell apoptosis detective kit [Annexin V-propidium iodide (PI)] was purchased from Jiangsu Kaiji Biotechnology Co., Ltd.

Cell culture. The human oral tongue squamous cell carcinoma CAL27 and SCC-15 cell lines were obtained from the American Type Culture Collection. Cells were cultured in DMEM with 10% FBS and 1% penicillin/streptomycin, and maintained in a humidified chamber of 95% air, 5% CO_2 and at 37˚C.

Cell viability assay. The cells were seeded into 96-well plates with $8x10^3$ cells/well and cultured overnight. After treated with different doses of PCA (0.5, 1.0 and 2.0 mg/ml) for 24 h, the cells were incubated with 10 μl CCK-8. After 2 h, a microplate reader was used to measure absorbance at 450 nm.

Colony formation assay. Aggregations of cells comprising a minimum of 50 cells were recognized as colonies. The cells were seeded into 6-well plates ($2x10^3$ cells/well) and treated with different concentrations (0, 0.0675, 0.125, 0.25, 0.5 and 1.0 mg/ml) of PCA at 37˚C for 2 weeks. Cell colonies were fixed with cold 100% methanol for 15 min at room temperature and stained with 0.1% crystal violet for 20 min at room temperature. Formed colonies were observed and captured by light microscope (IX51; Olympus Corporation). Colonies were quantified using Image J v1.8.0 (National Institutes of Health).

Intracellular reactive oxygen species (ROS) assay. In order to clarify whether the up-regulation of ROS levels in cells is the main reason for the inhibition of cell proliferation by PCA, ROS levels were measured in CAL27 cells and SCC-15 cells after co-administration of the ROS scavenger NAC and different concentrations of PCA in each group. The cells were washed with PBS and re-suspended in 10 μM fluorescent dye 2'-7'dichlorofluorescin diacetate (DCFH-DA). Next, cells were incubated in the dark for 30 min at 37˚C. The experimental procedure was completed according to the experimental step-by-step instructions of the ROS detection kit (Beyotime Institute of Biotechnology; cat. no. S0033S). After washing twice, the cells were observed and photographed under a fluorescence microscope, and intracellular ROS levels were semi-quantitatively detected in a flow cytometer (BD Biosciences). The results of cell flow analysis were statistically analyzed to obtain peak plots using FlowJo software v10.6.2 (BD Biosciences).

Wound healing assay. The cells were scratched using micro-pipette tips, and imaged using a microscope. The width of the scratch was measured and referred to as Wbefore. Then, the cells were treated with different concentrations (0, 0.5, 1.0 and 2.0 mg/ml) of PCA and starved with 2% serum DMEM. Cell migration was monitored and images were captures using a light microscope at 0, 6, 12, 24 and 48 h. In the present experiment, the distance of statistical cell migration was used as a quantitative method. By measuring the width of the same scratch, which is called Wafter, the migration distance is calculated by subtracting Wafter from Wbefore. The migration of the control was set as 100. The resultant scale on the image is 100 μm.

Reverse transcription-quantitative (RT-q)PCR. Total RNA was extracted using TRIzol (Invitrogen; Thermo Fisher Scientific, Inc.) reagent. PrimeScript™ RT Master Mix (Takara Bio, Inc.; cat. no. RR037A) according to the manufacturer's instructions. Relative mRNA levels were quantified with SYBR Green PCR Kit (Roche Diagnostics) and normalized to GAPDH using the following primers: GAPDH-F, 5'-AGAAGGCTGGGGCTCATTTG-3', and GAPDH-R, 5'-AGGGGCCATCCACAGTCTTC-3'; P21-F, 5'-GGAGACTCTCAGGGTCGAAA-3', P21-R, 5'-GGATTAGGGCTTCCTCTTGG-3'. The thermocycling parameters included: 40 cycles at 95˚C for 15 sec, 60˚C for 15 sec and 72˚C for 30 sec. Then another 10 min at 95˚C, 15 sec at 95˚C and 30 sec at 60˚C for 40 cycles. The mRNA levels of target genes were normalized to GAPDH and data of relative expression was quantified using the $2^{-\Delta\Delta cq}$ method (13). Data were obtained from triplicate experiments.

Mitochondrial membrane potential (ΔΨm) assay. ΔΨm was assessed using Rhodamine 123. Cells were incubated with 2 μM Rhodamine 123 in the dark for 30 min, and ΔΨm levels were detected in a flow cytometer (BD Biosciences). Mitochondrial fluorescence intensity-determined ΔΨm was assessed using High Content Screening (HCS) (14).

Cell cycle analysis. The cells were seeded into 6-well plates with $2x10^4$ cells/well and cultured overnight. The cells were harvested and fixed with 70% ethanol at -20˚C for 30 min. After washing with PBS, cells were stained (20 μg/ml PI, 200 μg/ml RNase). The cell cycle profiling was analyzed using a FACScan™ flow cytometer (BD Biosciences) using 488 nm excitation. The results of cell cycle analysis were statistically analyzed to obtain peak plots using FlowJo software v10.6.2 (BD Biosciences). Doublets were excluded from analysis, and 10,000 events were collected in the single-cell gate per sample.

Apoptosis analysis. The cells were seeded into 6-well plates with $2x10^4$ cells/well and cultured overnight. The cells were washed twice with cold PBS and added trypsin at 37˚C for 2 min for digestion. After exposure, the cells were harvested and stained with Annexin V-FITC and PI as recommended by the manufacturer. Samples were analyzed by FACScan™ flow cytometer (BD Biosciences). The results of apoptosis analysis were statistically analyzed by using FlowJo software v10.6.2 (BD Biosciences). The signals of early and late apoptotic cells were located in the lower and upper right quadrant of the resulting dot plot, respectively.

Western blotting. Total protein was extracted using RIPA buffer and a protease inhibitor cocktail (Beyotime Institute of Biotechnology) to prevent protein degradation. Cells were disrupted through sonication, ensuring complete lysis. A BCA protein assay kit (cat. no. P0012) was obtained from Beyotime Institute of Biotechnology and used following manufacturer's instructions for protein quantification. Cell lysates (30-50 μg) were separated by 12.5% SDS-PAGE and transferred onto PVDF membranes (Thermo Fisher Scientific, Inc.). After blocking with 5% non-fat milk in PBST buffer with 0.1% Tween for 1 h at room temperature, the blots were incubated with primary antibodies [anti-GAPDH (1:1,000), anti-p21 (1:1,000), anti-Bcl-2 (1:1,000), anti-Bax (1:1,000), anti-survivin (1:1,000), anti-LC3B (1:1,000), anti-p62 (1:1,000), anti-ERK (1:1,000), anti-p-ERK (1:1,000), anti-AKT (1:1,000.), anti-pAKT (1:1,000) and anti-PI3K (1:1,000) polyclonal antibodies] at 4˚C overnight. Membranes were then incubated with secondary antibodies (IRDye 800CW goat anti-rabbit IgG; 1:20,000] at room temperature for 1 h, and then detected using Odyssey infrared imaging system (LI-COR Biosciences). Densitometry were semi-quantified using Image J v1.8.0 (National Institutes of Health).

Immunofluorescence. The cells were seeded into 96-well plates with $8x10^3$ cells/well and cultured overnight. The cells were treated with different concentrations of PCA (0, 0.5, 1.0 and 2.0 mg/ml) for 24 h. Then, the cells were fixed with 4% paraformaldehyde for 15 min at room temperature, washed with PBS before permeabilization using 0.1% Triton X-100 for 10 min at room temperature. After washing with PBS, cells were blocked for 30 min in 5% BSA containment solution at 37˚C and then, incubated with primary antibody LC3B (1:400; Cell Signaling Technology, Inc.; cat. no. 3868) for 1 h at 37˚C, washed with PBS and incubated with fluorescently-labelled secondary antibody [FITC-conjugated Affinipure Goat Anti-Mouse IgG(H+L); 1:200; cat. no. A00003-1; Proteintech Group, Inc.] for 1 h at 37˚C. Finally, the nuclei were visualized by Hoechst33342 counterstaining for 5 min at room temperature. After washing with PBS, immunofluorescent cells were visualized using HSC and analyzed with the integrated Columbus (version 6.0) image data storage and analysis system (PerkinElmer, Inc.). The resultant scale on the image is 100 μm.

Statistical analysis. All data from three times experiments are presented as mean ± standard deviation. Statistical analyses were carried out using SPSS (version 16.0; IBM Corp.). Differences between two groups were assessed using a paired Student's t-test, and differences between ≥3 groups were assessed using one-way or two-way ANOVA followed by Bonferroni's post hoc test. $P<0.05$ and $P<0.01$ were considered to indicate statistically significant differences.

Results

Effects of PCA on cell viability and colony formation activity. To determine the effect of PCA on cell viability, CAL27 and SCC-15 cells were treated with different concentrations of PCA, and then a CCK-8 assay was carried out. PCA exhibited significant concentration-dependent anti-proliferative effects in CAL27 cells (Fig. 1A). The results showed that cell viability was significantly reduced at PCA concentration of 0.5 and 1.0 mg/ml ($P<0.05$). Cell activity was only 40% at the highest PCA concentration tested (2.0 mg/ml), compared with that in the control group ($P<0.01$). Similar results were observed in SCC-15 cells (Fig. 1B). PCA exhibited a significant inhibitory effect at 2 mg/ml on SCC-15 cells. These results indicate that CAL27 cells are more sensitive to PCA than SCC-15 cells.

Consequently, a colony formation assay was conducted to detect changes in the self-renewal ability of the two cell lines. Cell viability significantly decreased in a dose-dependent manner (Fig. 1C). Even at the lowest concentration (0.0675 mg/ml), PCA significantly inhibited CAL27 cell colony formation compared with the control. PCA had a similar inhibitory effect in SCC-15 cells (Fig. 1D). The anti-proliferative effects of PCA in SCC-15 cells were observed at the lowest dose (0.0675 mg/ml). These results are consistent those of the cell proliferation assays for both CAL27 and SCC-15 cells.

Effects of PCA on ΔΨm and intracellular ROS generation. Mitochondria are the center of the cellular oxidative respiratory chain as well as the center of apoptosis regulation. Decreased ΔΨm is known to be closely related to mitochondrial dysfunction (15). Therefore, the effects of PCA on mitochondrial function in human tongue squamous carcinoma cells was examined by HCS. CAL27 cells (Fig. 2A; left panels) and SCC-15 cells (Fig. 2B; left panels) treated with PCA were imaged under a light microscope; the mitochondrial membranes were stained with Rhodamine 123 (middle panels). Compared with the control group, the cells treated with PCA induced a reduction in the ΔΨm, suggesting that PCA induced a loss of ΔΨm in both CAL27 cells and SCC-15 cells. Moreover, it was observed that as the PCA concentration increased, the green fluorescence and number of cells gradually decreased. The results are consistent with those of the CCK-8 assay results.

DCFH-DA was used to assess ROS production to investigate whether ROS would be generated in CAL27 cells after PCA treatment. The intracellular ROS levels in CAL27 cells increased significantly after PCA treatment (Fig. 2C and E). These effects were dose dependent. However, this increase in DCFH-DA-based fluorescence was not inhibited by pretreatment with the ROS scavenger N-acetyl-L-cysteine (NAC), which did not reduce the PCA-induced increase in fluorescence. These results indicate that ROS production was not the main cause of the inhibited proliferation of CAL27 cells exposed to PCA.

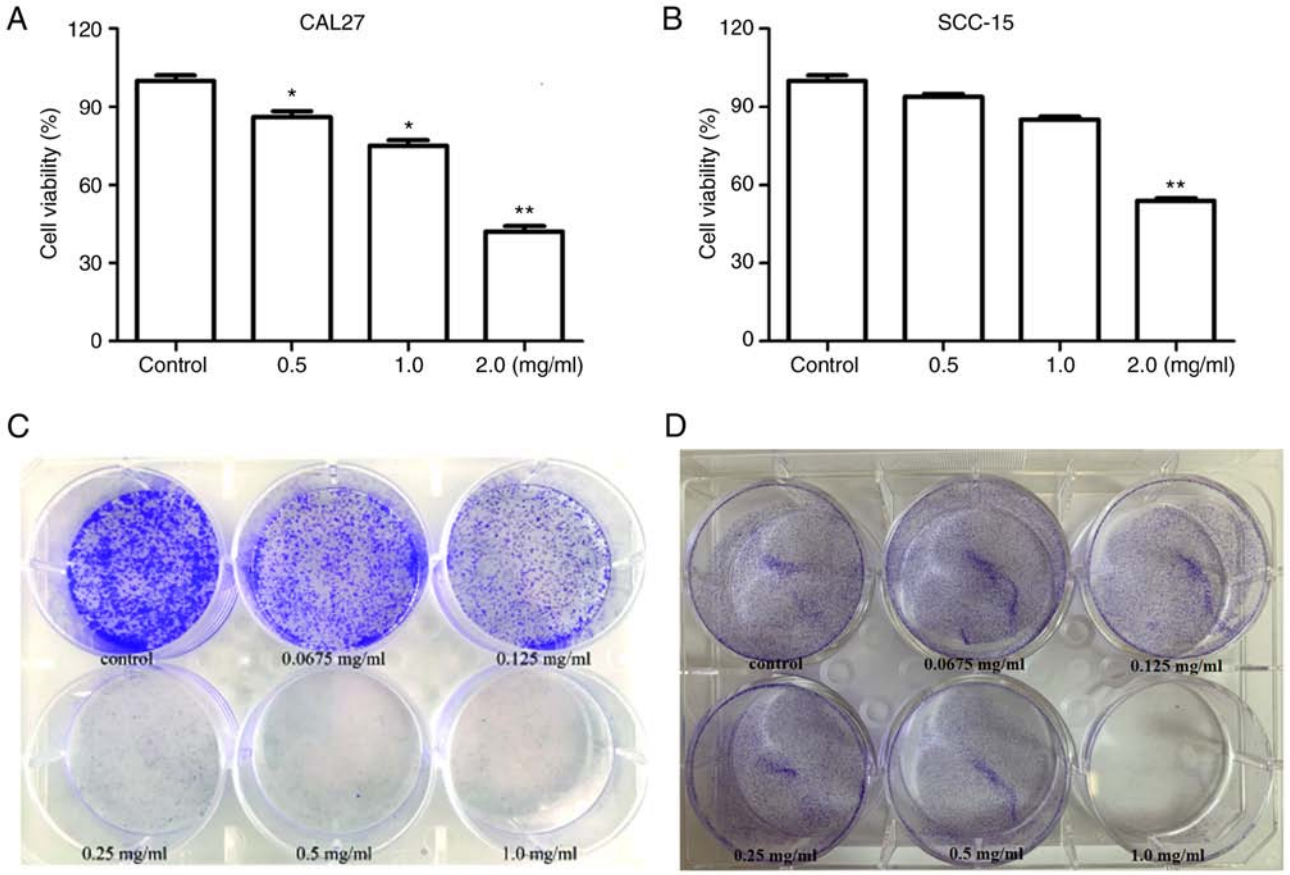

Figure 1. Effects of PCA on cell viability and colony formation activity. Cell viability was analyzed using the Cell Counting Kit-8 assay. (A) CAL27 and (B) SCC-15 cells were incubated with different concentrations of PCA (0, 0.5, 1.0 and 2.0 mg/ml). The data are shown as mean ± SD. *P<0.05, **P<0.01 vs. control. Colony formation assays were performed to investigate the effects of PCA on proliferation. (C) CAL27 and (D) SCC-15 cells incubated with PCA for 2 weeks. The colonies were stained and counted. PCA, procaine. All experiments were assessed using a paired Student's t-test for analysis.

Similar results were found in SCC-15 cells (Fig. 2D and F). A significant dose-dependent loss of ΔΨm was observed in SCC-15 cells after PCA treatment (Fig. 2B). Furthermore, NAC partially reversed PCA-induced ROS production, which is consistent with the results obtained in CAL27 cells (NAC + 1 mg/ml PCA; *P<0.05; Fig. 2E).

Effects of PCA on cell cycle. To elucidate the mechanism by which PCA inhibits cell proliferation, the cell cycle distribution was examined using flow cytometry. The G0/G1 phase population was reduced in CAL27 cells after PCA treatment, whereas the G2/M phase cell population was significantly increased, suggesting that PCA caused G2/M phase arrest in CAL27 cells (Fig. 3A and C). Notably, no remarkable G2/M arrest was observed at the highest concentration of PCA (2 mg/ml), although an increase in the S phase cell population was observed. This indicated that the cells were inhibited in the S phase at a high PCA dose.

Similar results were observed in SCC-15 cells (Fig. 3B and D) as PCA induced G2/M phase arrest. The potential mechanisms by which PCA induced G2/M phase arrest in CAL27 cells were further explored.

RT-qPCR was performed to analyze the expression of the cyclin-dependent kinase inhibitor p21, which is related to S phase arrest. p21 mRNA expression levels significantly increased with increasing PCA concentrations (*P<0.05, **P<0.01; Fig. 3E). Moreover, p21 protein expression increased in a PCA dose-dependent manner, which is consistent with the RT-qPCR results (Fig. 3F and G).

Effects of PCA on cell migration. The effects of PCA on SCC-15 and CAL27 cells were compared using CCK8, immunofluorescence and cell proliferation assays. The results were found to be similar for both cell lines. In addition, the results of the CCK8 assay, colony formation assay, intracellular ROS assay, ΔΨm assay, cell cycle analysis and immunofluorescence analysis all revealed that CAL27 cells are more sensitive to PCA than SCC-15 cells. Therefore, for subsequent in-depth mechanistic studies, CAL27 cells were focused on. In the present experiment, the effect of PCA on CAL27 cell migration was investigated in greater depth. A number of drugs affect both cell morphology and migration. To determine the inhibitory effects of PCA on cell migration, a wound healing assay using CAL27 cells was performed (Fig. 4A and B). PCA inhibited cell migration in a concentration- and time-dependent manner. The scratch area increased with increasing PCA concentration, especially at 24 and 48 h. Compared with the control group, the scratching area healed with 2.0 mg/ml PCA (*P<0.05, **P<0.01), which showed that PCA significantly inhibited the cell healing rate.

Effects of PCA on apoptosis. PCA blocked cell proliferation and induced growth arrest in CAL27 cells. To further clarify

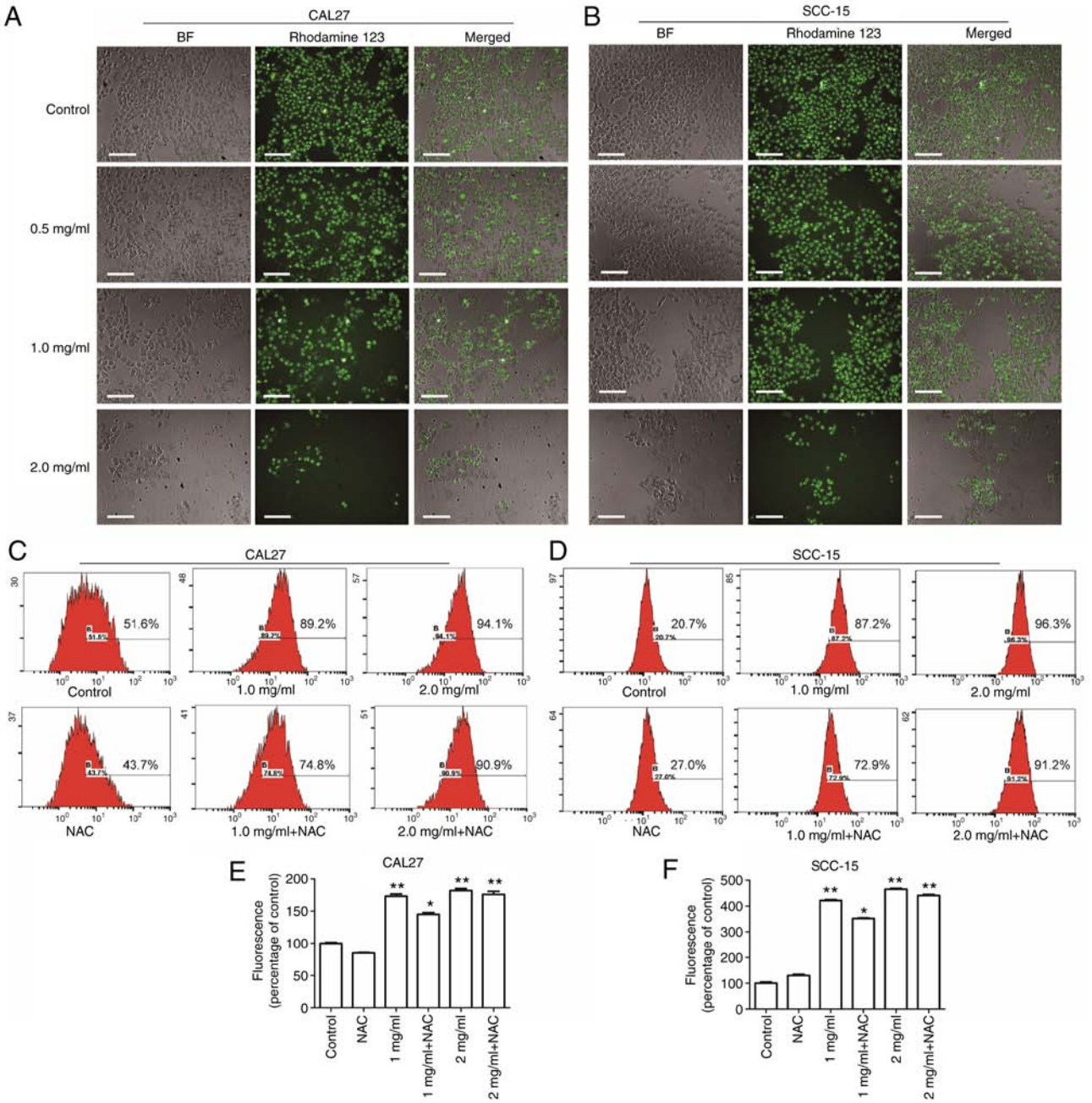

Figure 2. Effects of PCA on mitochondrial damage. (A) CAL27 and (B) SCC-15 cells were treated with different concentrations of PCA and stained by Rhodamine 123. Mitochondrial membrane potential was determined by High Content Screening. (C) CAL27 and (D) SCC-15 cells were preincubated with or without NAC before exposure to PCA for 24 h. Percentage changes in intracellular reactive oxygen species generation were measured by flow cytometry. Quantitative analysis data of (E) CAL27 and (F) SCC-15 (*P<0.05, **P<0.01 vs. control). PCA, procaine; NAC, N-acetyl-L-cysteine. All experiments were assessed using one-way ANOVA for analysis.

the underlying mechanisms, CAL27 cells were treated with different concentrations of PCA, dual-stained with Annexin-V-FITC and PI and analyzed using flow cytometry. The early and late apoptotic rates of PCA-treated cells were observed in a dose-dependent manner (Fig. 5A). At the highest concentration tested (2 mg/ml), ~11.0% of the cells underwent late apoptosis compared with 1.6% of the control cells. These results suggest that PCA treatment increased apoptosis in a dose -and time-dependent manner in CAL27 cells.

The effect of PCA on anti-apoptotic (Bcl-2) and apoptotic (Bax) protein expression was then analyzed. As it was anticipated, Bcl-2 expression was significantly suppressed (**P<0.01), whereas Bax expression was slightly increased (*P<0.05), suggesting that PCA-mediated inhibition of proliferation occurred through apoptosis induction (Fig. 5B and C).

The effects of PCA on the ERK and PI3K/AKT signaling pathways were examined to determine which signaling pathways play important roles in PCA-induced apoptosis. Both ERK and p-ERK protein expression levels were significantly reduced in a dose-dependent manner in PCA-treated CAL27 cells compared with the control group (Fig. 5C and D). These results suggest that PCA inhibits the ERK signaling pathway. Moreover, with increasing concentrations of PCA, both p-AKT and PI3K expression levels were decreased,

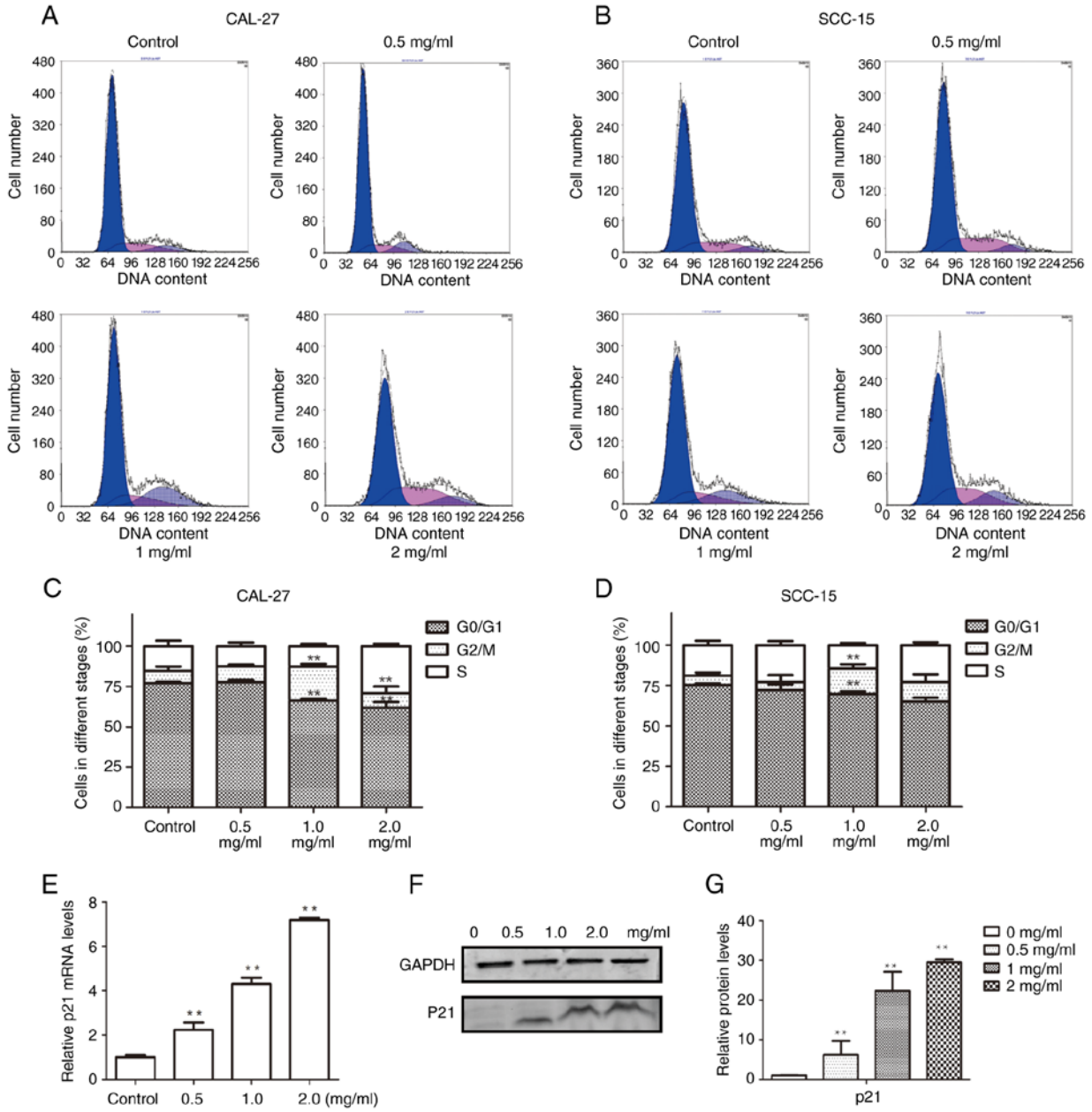

Figure 3. Effects of PCA on cell cycle. Cells were treated with different concentrations of PCA for 24 h. (A) CAL27 and (B) SCC-15 cells cycle distribution determined by flow cytometry. Statistical analysis of (C) CAL27 and (D) SCC-15 cells cycle phases. (E) The relative mRNA expression of p21 was detected by reverse transcription-quantitative PCR on CAL27 cells. (F) The p21 protein expression in CAL27 cells was detected by western blotting. GAPDH was used to normalize protein levels. (G) Quantification of p21 protein expression compared with that of the control group (mean ± SD; n=3). **P<0.01. PCA, procaine. All experiments were assessed using one-way ANOVA for analysis.

indicating that PCA also inhibits the PI3K/AKT signaling pathway.

Effects of PCA on cell autophagy. The LC3 protein expression level, a marker of autophagy, was determined to investigate whether autophagy participates in the effect of PCA on CAL27 cell proliferation. The cell nucleus was stained with Hoechst33342, whereas autophagosomes were visualized as FITC-labeled LC3B (Fig. 6A). With an increase in PCA concentration, the number of live cells gradually decreased, and the intensity of green fluorescence gradually increased. Moreover, green fluorescence was mainly distributed in the cytoplasm and was not co-localized with the nucleus. These results indicated that PCA induced autophagy. Western blotting showed similar results. The LC3II/I expression levels increased in a concentration-dependent manner in PCA-pretreated CAL27 cells compared with the control group, suggesting that PCA induces autophagy in CAL27 cells (Fig. 6B and C). To determine whether PCA could induce complete autophagy, the levels of the autophagy substrate p62 were examined. The p62 protein expression levels also showed a significant concentration-dependent increase, suggesting that autophagy flux might be inhibited by PCA.

Effects of autophagy on apoptosis induced by PCA. Autophagy is regarded as a double-edged sword in tumor

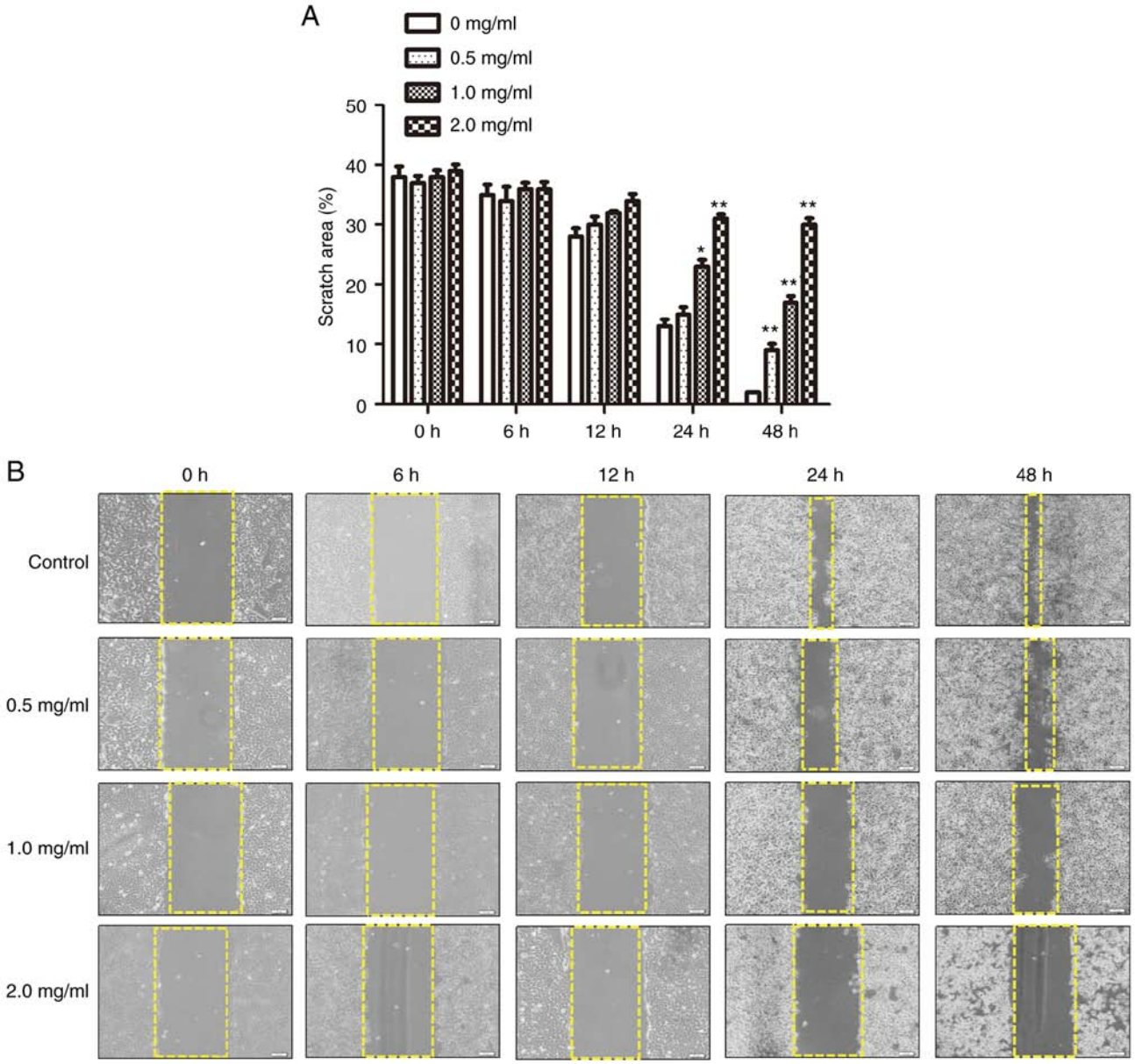

Figure 4. Effects of PCA on cell migration. Cells were scratched by tips and exposed at PCA for different time periods. (A) Scratching areas were calculated using Image J (*P<0.05, **P<0.01). Scale bar, 100 μm. (B) Cells scratching wounds were observed by microscope. Original magnification, x200. PCA, procaine. All experiments were assessed using two-way ANOVA for analysis.

development and treatment because it kills tumor cells and protects them from injury (16,17). To clarify the role of autophagy in PCA-induced apoptosis, changes in autophagic flux were examined by treating cells with the lysosomal inhibitor CQ alone or in combination with PCA and measuring LC3II/I and p62 expression levels using western blotting. PCA combined with CQ significantly enhanced the transformation of LC3I to LC3II in CAL27 cells (Fig. 6D and E). It was also observed that the addition of CQ had no significant effect on the change in p62 expression.

Next, it was observed that compared with PCA-treated cells, PCA combined with CQ significantly reduced cell activity for 24 h (Fig. 6F). The apoptotic effects of PCA combined with CQ were then investigated. A total of ~34.3% of CAL27 cells demonstrated late apoptosis at the highest dose (2 mg/ml) of PCA combined with CQ compared with 10.7% of the cells treated with PCA alone, indicating that the apoptosis rate in cells treated with PCA combined with CQ was higher than that in cells treated with PCA alone (Fig. 6I).

Similarly, protein expression levels were detected in the surviving cells. Compared with the PCA-treated group, survivin protein expression was significantly reduced in the PCA + CQ group (Fig. 6H). These results suggest that the inhibition of autophagy could enhance the sensitivity of PCA.

Discussion

Novel drugs often take decades to transition from laboratories to clinical application. Therefore, an increasing number of researchers are turning their attention to the 'new use of old drugs'. 'Old drugs' are drugs that have been marketed or are undergoing clinical trials, and 'new use' refers to

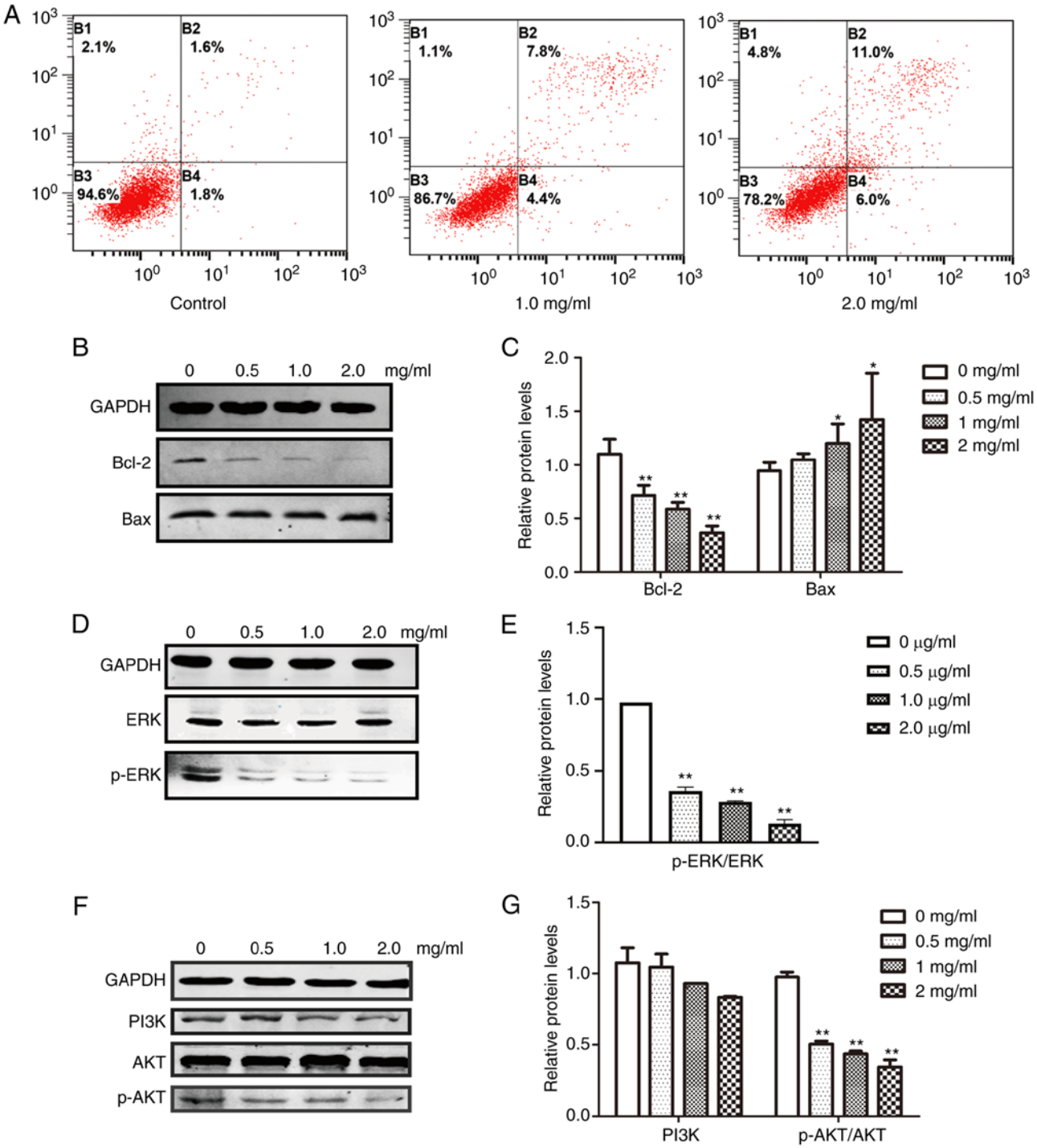

Figure 5. Effects of PCA on cell apoptosis. Cells were treated with different concentrations of PCA for 24 h. (A) Effects of PCA on cell apoptosis were detected by flow cytometry. (B) Expression levels of cell apoptosis-regulated proteins determined by western blotting. (C) Quantification of cell apoptosis-regulated proteins. (D) Expression levels of ERK signaling pathway proteins determined by western blotting. (E) Quantification of ERK signaling pathway proteins. (F) Expression levels of PI3K/AKT signaling pathway proteins determined by western blotting. (G) Quantification of PI3K/AKT signaling pathway proteins compared with the control group. In Fig. 5B, D and F, GAPDH was used as the loading control. PCA, procaine; p, phosphorylated. All experiments were assessed using one-way or two-way ANOVA for analysis. *P<0.05, **P<0.01.

the discovery of new indications and their use in disease treatment (18). For instance, aspirin has been used as an antipyretic and analgesic for >100 years. Owing to more in-depth clinical research, researchers have discovered that aspirin plays a role in the prevention and treatment of cardiovascular diseases and also in cancer prevention and treatment (19,20). Another example is the metformin, which reduces blood sugar, promotes antitumor activity and also treats abnormal metabolic diseases (21,22). A previous study demonstrated that metformin can also regulate the metabolic flux of stem cells in the stomach and promote their differentiation into gastric parietal cells that produce gastric acid, protecting the stomach (23). Several recent studies have reported that anesthetics may have antitumor effects, which has aroused

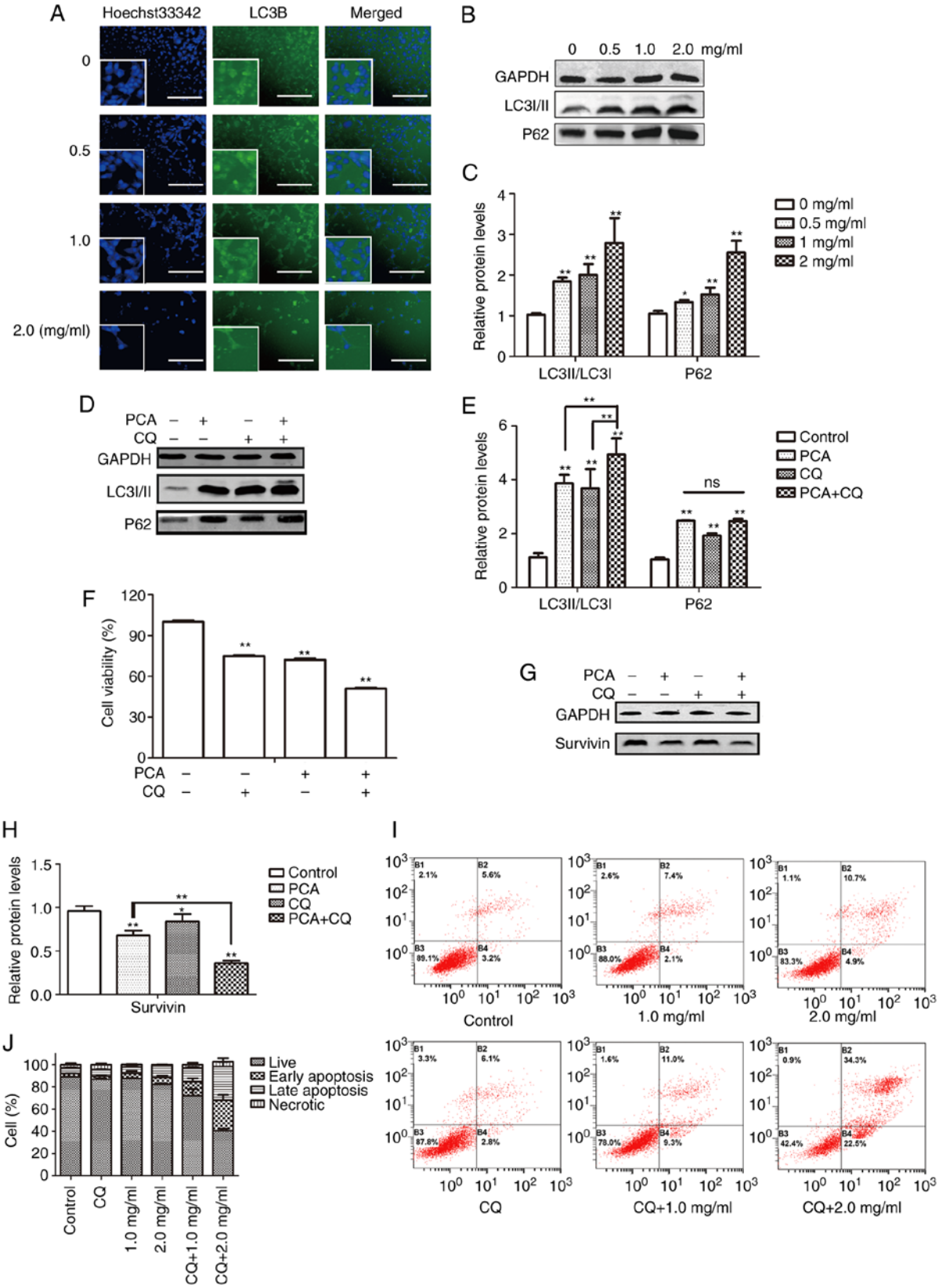

Figure 6. Effects of PCA on cell autophagy. (A) Cells were treated with PCA for 24 h. Cells expressing LC3B were stained by FITC. Cells were stained with Hoechst33342, and fluorescence was visualized (scale bar, 100 μm) Original magnifications, x200. Higher magnification displayed in the lower left corner (x400). Cells were preincubated with or without CQ before exposure to PCA for 24 h. (B) Expression levels of p62 and LC3 in absence of CQ determined by western blotting. (C) Quantification of p62 and LC3 expression levels in absence of CQ. (D) Expression levels of p62 and LC3 in presence of CQ determined by western blotting. (E) Quantification of p62 and LC3 expression levels in presence of CQ. (F) Effects of PCA on cell viability in presence of CQ were determined using a Cell Counting Kit-8 assay. (G) Expression levels of cell apoptosis-regulated proteins determined by western blotting. (H) Quantification of survivin expression. (I) Effects of PCA on cell apoptosis in presence of CQ were determined by flow cytometry. (J) Summary of the apoptosis assay results displayed as percentages of cells in different cell death stages: Live cells, early apoptosis, late apoptosis and necrosis. In Fig. 6B, D and G, GAPDH was used as the loading control (*P<0.05, **P<0.01). PCA, procaine; CQ, chloroquine; ns, not significant. All experiments were assessed using one-way or two-way ANOVA for analysis.

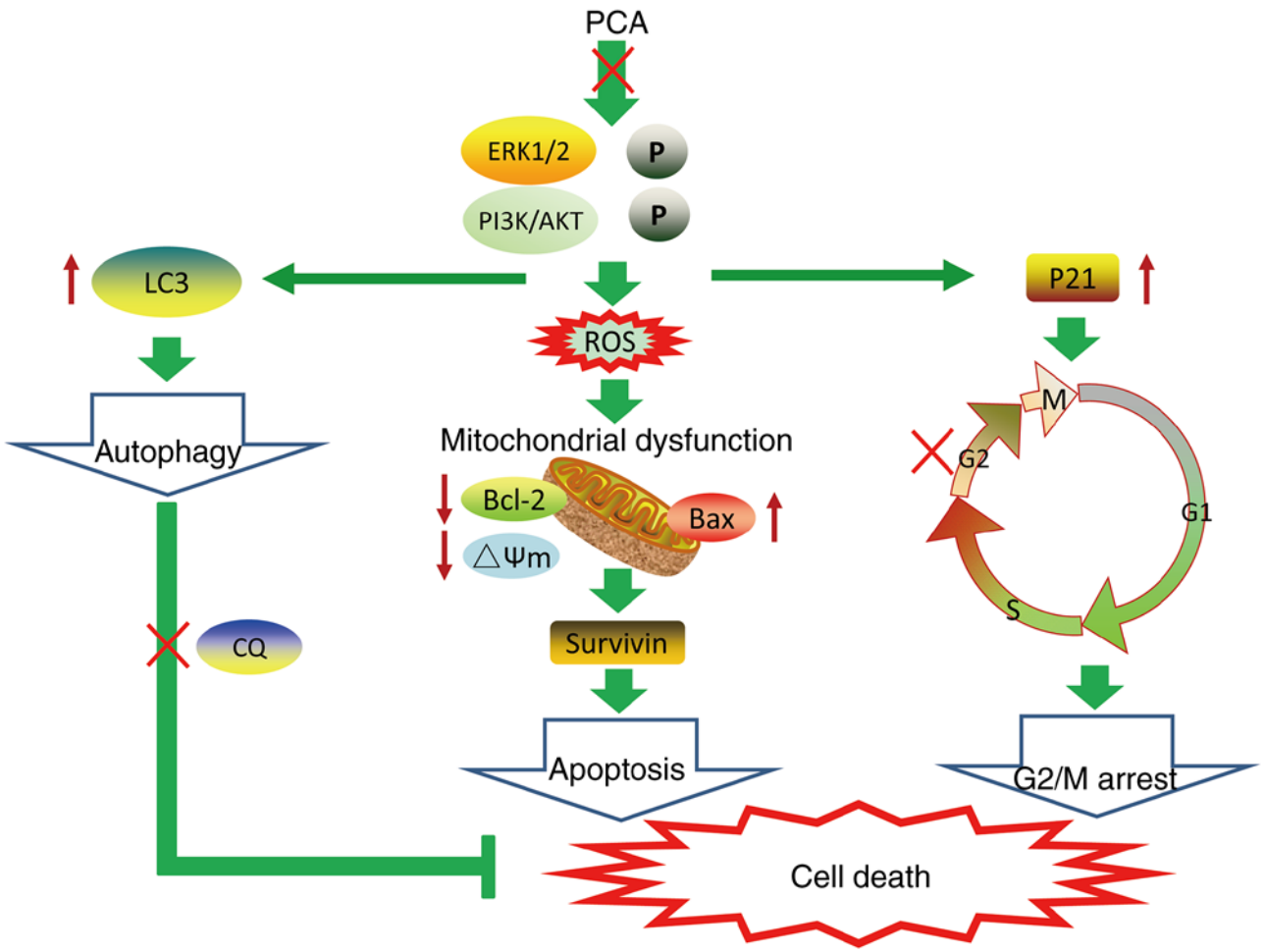

Figure 7. Schematic model for PCA-induced cell death. PCA, procaine; CQ, chloroquine; ROS, reactive oxygen species; p, phosphorylated; ΔΨm, mitochondrial membrane potential.

great interest. For example, Chen *et al* (24) found that propofol exerts an antitumor effect by inhibiting autophagic flux in HeLa cells (24). Another study showed that 400 mM lidocaine inhibited the proliferation of CAL27 cells with high EGFR expression without cytotoxicity (25). As a representative anesthetic, PCA has also shown antitumor effects in different types of cancer, including lung (26), colon (13) and breast (27) cancer. In the aforementioned studies, the range of antitumor PCA doses was micromolar to millimolar; 2 μM (26), 2 mM (12) and 10 mM (26). In the present study, the PCA dose associated with significant antitumor properties was 1-2 mg/ml *in vitro*, which is equivalent to 8.5 mM and is roughly similar to the dose used to induce PCA antitumor activity in the aforementioned published studies. Meanwhile, it was also observed that the FDA-approved dose of PCA for injection is 1 or 2%, which is ~10 mg/ml. This dose differs from the doses used in the present study. Some 'old drugs', which have been approved for clinical use, are used as 'new efficacy drugs' by altering the dose, such as with aspirin and metformin. If PCA is to be used clinically as an antitumor agent in the future, further animal and clinical trials are required.

In the current study, it was shown that PCA had different antiproliferative effects by investigating two OSCC cell lines. CAL27 cells were more sensitive to PCA treatment than SCC-15 cells, indicating that the *in vitro* inhibitory effects of PCA depend on the cancer cell line.

Tumorigenesis is a phenomenon of uncontrolled cell proliferation caused by abnormal cell cycle regulation; therefore, blocking the cell cycle is usually an important means of tumor treatment (28). The results of the present study showed that PCA induced G2/M arrest and upregulated the expression of the cyclin 1 kinase inhibitor p21, which is known to inhibit mammalian cell proliferation, induce cell cycle arrest and inhibit the cyclin-cdk complex (29). These results indicate that p21 may play a key regulatory role during PCA-induced G2/M arrest in CAL27 cells.

The mitochondrial pathway is a main signaling pathway that induces apoptosis (30). Numerous anticancer drugs exert antitumor effects by activating the mitochondrial apoptosis pathway. The anti-apoptotic protein Bcl-2 and the pro-apoptotic protein Bax control cell apoptosis by regulating mitochondrial membrane permeability (31). The present study found that PCA downregulated Bcl-2 and upregulated Bax expression, caused ROS explosion in cells and decreased the $\Delta\Psi m$, suggesting that PCA may induce CAL27 cell apoptosis by activating the mitochondrial pathway.

In addition to the classic antitumor mechanisms, such as apoptosis induction and cell cycle arrest, it was observed that PCA can induce autophagy. Autophagy is a double-edged sword

that promotes and inhibits tumorigenesis (31-34). Therefore, the regulation of autophagy is expected to become a novel method for tumor prevention and treatment. LC3 and p62 are markers of autophagosome formation and degradation, respectively, and are used to detect autophagic flux (35). The increase in LC3II levels represents an increase in autophagosomes or the blockade of autophagosomal maturation and completion of the autophagy pathway. For example, cetuximab induces p27 accumulation and type II LC3B induction in retinoblastoma cells (36). Recent studies have shown that autophagy preferentially degrades p62 as a particular substrate (37,38). The total p62 expression level was negatively associated with autophagic activity. Autophagosomes are intermediate structures involved in dynamic cellular autophagy. At any point in time, the autophagosome production rate and the rate at which autolysosomes are converted into autolysosomes are balanced (39). It was shown that PCA induced LC3II protein accumulation and increased p62 levels. To demonstrate this, the well-known autophagy inhibitor CQ was used to detect autophagy flux. CQ can inhibit late autophagy by increasing lysosomal pH and inhibiting lysosomal enzyme chelation, thereby preventing autophagic degradation (11). The results showed that LC3II levels, after CQ combined with PCA were significantly higher than LC3II levels induced by PCA or CQ alone. These data indicate that PCA can cause the accumulation of autophagosomes, which cannot be ignored. The accumulation of autophagosomes induced by PCA may be due to an increase in autophagosome generation caused by early autophagy activation, or the blocking of autophagosomal clearance caused by late autophagy inhibition. This question needs to be answered in the future (40).

Recently, the ERK pathway has become an attractive therapeutic target, and several drugs targeting this pathway have shown promise in clinical trials. PCA reportedly affects HCT 116 cell proliferation, migration and apoptosis and inactivates the ERK pathway by regulating RhoA (13). Moreover, Li *et al* (13) revealed that PCA inhibited MG63 cells viability by upregulating microRNA-133b, thereby inactivating the AKT/ERK pathway. The current study also confirmed that PCA produces antitumor effects by reducing p-ERK in CAL27 cells, suggesting that PCA may play an inhibitory role in various malignant tumors by inhibiting the ERK signaling pathway.

In apoptosis-related pathways, specific signals and growth factors activate the PI3K/AKT pathway, which regulates cell proliferation, differentiation, metabolism, migration and other biological processes. For example, Yang *et al* (41) found that oridonin induced G2/M phase arrest and apoptosis and inhibited OSCC cell proliferation by inhibiting the PI3K/AKT signaling pathway. The results of the current study further confirmed that PCA inhibited proliferation, and induced cell cycle arrest and apoptosis in CAL27 cells by inhibiting PI3K/AKT phosphorylation.

The current study has some limitations. *In vivo* experiments are required to elucidate the antitumor activity and mechanism of PCA. Therefore, besides OSCC cell lines, nude mice xenografts or clinical samples are worthy for validation. In addition, although no study has yet demonstrated the role of PCA in the tumor microenvironment, considering the network effects in the organism, hypothesizing that PCA may be involved in the progression of OSCC by modulating immune infiltration through interactions with immune cells, vasculature and nerves is reasonable. These findings warrant further study in the future.

A schematic model of PCA-induced cell death is shown in Fig. 7. The findings of the present study demonstrate that PCA inhibits cell proliferation and migration by impairing mitochondrial function and inducing G2/M cycle arrest and apoptosis. The inhibitory effects of PCA on CAL27 cell growth may be dependent on PI3K/AKT and ERK pathway inhibition. Meanwhile, it was shown that PCA elicited autophagy and blocked autophagic flux. The combination of PCA and the autophagy inhibitor CQ enhanced CAL27 cell sensitivity to PCA. The results of the current study indicate the potential PCA as a novel drug against tongue squamous cell carcinoma.

Acknowledgements

Not applicable.

Funding

The present study was funded by the Jilin Provincial Department of Finance (grant no. 2023SCZ64), the National Natural Science Foundation of China (grant no. 81903881), and the Department of Science and Technology of Jilin Province (grant nos. 20190103086JH and 20200201398JC).

Availability of data and materials

The data generated in the present study may be requested from the corresponding author.

Authors' contributions

CZ and MH performed the experiments. NS, LY and TZ analyzed the data. CZ and MH wrote the manuscript. TZ and XW designed and supervised the study. MH and XW confirm the authenticity of all the raw data. All authors read and approved the final version of the manuscript.

Ethics approval and consent to participate

Not applicable.

Patient consent for publication

Not applicable.

Competing interests

The authors declare that they have no competing interests.

References

1. Omura K: Current status of oral cancer treatment strategies: Surgical treatments for oral squamous cell carcinoma. Int J Clin Oncol 19: 423-430, 2014.
2. Tampa M, Mitran MI, Mitran CI, Sarbu MI, Matei C, Nicolae I, Caruntu A, Tocut SM, Popa MI, Caruntu C and Georgescu SR: Mediators of inflammation-A potential source of biomarkers in oral squamous cell carcinoma. J Immunol Res 12: 1061780, 2018.

3. Lien JC, Lin MW, Chang SJ, Lai KC, Huang AC, Yu FS and Chung JG: Tetrandrine induces programmed cell death in human oral cancer CAL 27 cells through the reactive oxygen species production and caspase-dependent pathways and associated with beclin-1-induced cell autophagy. Environ Toxicol 32: 329-343, 2017.
4. Ng JH, Iyer NG, Tan MH and Edgren G: Changing epidemiology of oral squamous cell carcinoma of the tongue: A global study. Head Neck 39: 297-304, 2017.
5. Chu H, Li Z, Gan Z, Yang Z, Wu Z and Rong M: LncRNA ELF3-AS1 is involved in the regulation of oral squamous cell carcinoma cell proliferation by reprogramming glucose metabolism. Onco Targets Ther 12: 6857-6863, 2019.
6. Tan Y, Wang Z, Xu M, Li B, Huang Z, Qin S, Nice EC, Tang J and Huang C: Oral squamous cell carcinomas: State of the field and emerging directions. Int J Oral Sci 15: 44, 2023.
7. Adelstein D, Gillison ML, Pfister DG, Spencer S, Adkins D, Brizel DM, Burtness B, Busse PM, Caudell JJ, Cmelak AJ, *et al*: NCCN guidelines insights: Head and neck cancers, version 2.2017. J Natl Compr Canc Netw 15: 761-770, 2017.
8. Mouw KW, Haraf DJ, Stenson KM, Cohen EE, Xi X, Witt ME, List M, Blair EA, Vokes EE and Salama JK: Factors associated with long-term speech and swallowing outcomes after chemoradiotherapy for locoregionally advanced head and neck cancer. Arch Otolaryngol Head Neck Surg 136: 1226-1234, 2010.
9. Li YC, Wang Y, Li DD, Zhang Y, Zhao TC and Li CF: Procaine is a specific DNA methylation inhibitor with anti-tumor effect for human gastric cancer. J Cell Biochem 119: 2440-2449, 2018.
10. Schumann NAB, Mendonça AS, Silveira MM, Vargas LN, Leme LO, de Sousa RV and Franco MM: Procaine and S-Adenosyl-l-Homocysteine affect the expression of genes related to the epigenetic machinery and change the DNA methylation status of in vitro cultured bovine skin fibroblasts. DNA Cell Biol 39: 37-49, 2020.
11. Villar-Garea A, Fraga MF, Espada J and Esteller M: Procaine is a DNA-demethylating agent with growth-inhibitory effects in human cancer cells. Cancer Res 63: 4984-4989, 2003.
12. Tada M, Imazeki F, Fukai K, Sakamoto A, Arai M, Mikata R, Tokuhisa T and Yokosuka O: Procaine inhibits the proliferation and DNA methylation in human hepatoma cells. Hepatol Int 1: 355-364, 2007.
13. Li C, Gao S, Li X, Li C and Ma L: Procaine inhibits the proliferation and migration of colon cancer cells through inactivation of the ERK/MAPK/FAK pathways by regulation of RhoA. Oncol Res 26: 209-217, 2018.
14. Chen X, Li LY, Jiang JL, Li K, Su ZB, Zhang FQ, Zhang WJ and Zhao GQ: Propofol elicits autophagy via endoplasmic reticulum stress and calcium exchange in C2C12 myoblast cell line. PLoS One 13: e0197934, 2018.
15. Zhao X, Qi T, Kong C, Hao M, Wang Y, Li J, Liu B, Gao Y and Jiang J: Photothermal exposure of polydopamine-coated branched Au-Ag nanoparticles induces cell cycle arrest, apoptosis, and autophagy in human bladder cancer cells. Int J Nanomedicine 13: 6413-6428, 2018.
16. Li X, He S and Ma B: Autophagy and autophagy-related proteins in cancer. Mol Cancer 19: 12, 2020.
17. Marsh T and Debnath J: Autophagy suppresses breast cancer metastasis by degrading NBR1. Autophagy 16: 1164-1165, 2020.
18. Nosengo N: Can you teach old drugs new tricks? Nature 534: 314-316, 2016.
19. Sperling CD, Verdoodt F, Aalborg GL, Dehlendorff C, Friis S and Kjaer SK: Low-dose aspirin use and endometrial cancer mortality-a Danish nationwide cohort study. Int J Epidemiol 49: 330-337, 2020.
20. Guo CG, Cheung KS, Zhang F, Chan EW, Chen L, Wong IC and Leung WK: Incidences, temporal trends and risks of hospitalisation for gastrointestinal bleeding in new or chronic low-dose aspirin users after treatment for Helicobacter pylori: A territory-wide cohort study. Gut 69: 445-452, 2020.
21. Guardado-Mendoza R, Salazar-López SS, Álvarez-Canales M, Farfán-Vázquez D, Martínez-López YE, Jiménez-Ceja LM, Suárez-Pérez EL, Angulo-Romero F, Evia-Viscarra ML, Montes de Oca-Loyola ML, *et al*: The combination of linagliptin, metformin and lifestyle modification to prevent type 2 diabetes (PRELLIM). A randomized clinical trial. Metabolism 104: 154054, 2020.
22. Dong TS, Chang HH, Hauer M, Lagishetty V, Katzka W, Rozengurt E, Jacobs JP and Eibl G: Metformin alters the duodenal microbiome and decreases the incidence of pancreatic ductal adenocarcinoma promoted by diet-induced obesity. Am J Physiol Gastrointest Liver Physiol 317: G763-G772, 2019.
23. Miao ZF, Adkins-Threats M, Burclaff JR, Osaki LH, Sun JX, Kefalov Y, He Z, Wang ZN and Mills JC: A Metformin-Responsive metabolic pathway controls distinct steps in gastric progenitor fate decisions and maturation. Cell Stem Cell 26: 910-925.e6, 2020.
24. Chen X, Li K and Zhao G: Propofol Inhibits HeLa cells by impairing autophagic flux via AMP-Activated Protein Kinase (AMPK) activation and endoplasmic reticulum stress regulated by calcium. Med Sci Monit 24: 2339-2349, 2018.
25. Sakaguchi M, Kuroda Y and Hirose M: The antiproliferative effect of lidocaine on human tongue cancer cells with inhibition of the activity of epidermal growth factor receptor. Anesth Analg 102: 1103-1107, 2006.
26. Ma XW, Li Y, Han XC and Xin QZ: The effect of low dosage of procaine on lung cancer cell proliferation. Eur Rev Med Pharmacol Sci 20: 4791-4795, 2016.
27. Chen C, Wang N, Huang T, Cheng G, Hu Y, Wang B, Zhang Y and Wang C: Chloroprocaine antagonizes progression of breast cancer by regulating LINC00494/miR-3619-5p/MED19 axis. J Biochem Mol Toxicol 38: e23524, 2024.
28. Lin AB, McNeely SC and Beckmann RP: Achieving precision death with cell-cycle inhibitors that target DNA replication and repair. Clin Cancer Res 23: 3232-3240, 2017.
29. Wang Z, Sturgis EM, Zhang F, Lei D, Liu Z, Xu L, Song X, Wei Q and Li G: Genetic variants of p27 and p21 as predictors for risk of second primary malignancy in patients with index squamous cell carcinoma of head and neck. Mol Cancer 11: 17, 2012.
30. Fulda S and Debatin KM: Extrinsic versus intrinsic apoptosis pathways in anticancer chemotherapy. Oncogene 25: 4798-4811, 2006.
31. Pfeffer CM and Singh ATK: Apoptosis: A target for anticancer therapy. Int J Mol Sci 19: 448, 2018.
32. Gao W, Wang X, Zhou Y, Wang X and Yu Y: Autophagy, ferroptosis, pyroptosis, and necroptosis in tumor immunotherapy. Signal Transduct Target Ther 7: 196, 2022.
33. Levine B and Kroemer G: Autophagy in the pathogenesis of disease. Cell 132: 27-42, 2008.
34. Mizushima N and Komatsu M: Autophagy: Renovation of cells and tissues. Cell 147: 728-741, 2011.
35. Zhou J, Hu SE, Tan SH, Cao R, Chen Y, Xia D, Zhu X, Yang XF, Ong CN and Shen HM: Andrographolide sensitizes cisplatin-induced apoptosis via suppression of autophagosome-lysosome fusion in human cancer cells. Autophagy 8: 338-349, 2012.
36. Okuyama K, Suzuki K, Naruse T, Tsuchihashi H, Yanamoto S, Kaida A, Miura M, Umeda M and Yamashita S: Prolonged cetuximab treatment promotes p27Kip1-mediated G1 arrest and autophagy in head and neck squamous cell carcinoma. Sci Rep 11: 5259, 2021.
37. Lamark T, Svenning S and Johansen T: Regulation of selective autophagy: The p62/SQSTM1 paradigm. Essays Biochem 61: 609-624, 2017.
38. Deng Z, Lim J, Wang Q, Purtell K, Wu S, Palomo GM, Tan H, Manfredi G, Zhao Y, Peng J, *et al*: ALS-FTLD-linked mutations of SQSTM1/p62 disrupt selective autophagy and NFE2L2/NRF2 anti-oxidative stress pathway. Autophagy 16: 917-931, 2020.
39. Mizushima N, Yoshimori T and Levine B: Methods in mammalian autophagy research. Cell 140: 313-326, 2010.
40. Mizushima N, Yamamoto A, Matsui M, Matsui M, Yoshimori T, Yoshimori T and Ohsumi Y: In vivo analysis of autophagy in response to nutrient starvation using transgenic mice expressing a fluorescent autophagosome marker. Mol Biol Cell 15: 1101-1111, 2004.
41. Yang J, Ren X, Zhang L, Li Y, Cheng B and Xia J: Oridonin inhibits oral cancer growth and PI3K/Akt signaling pathway. Biomed Pharmacother 100: 226-232, 2018.